https://doi.org/10.5194/egusphere-2022-1495
Preprint. Discussion started: 1 March 2023

Tidal dynamics limit river plastic transport

Louise D.M. Schreyers[1], Tim H.M. van Emmerik[1], Khiet Bui[2], Khoa Van Le Thi[1,3], Bart Vermeulen[1], Hong.-Q. Nguyen[2], and Martine van der Ploeg[1]

[1]Hydrology and Quantitative Water Management Group, Wageningen University and Research, The Netherlands
[2]Institute for Circular Economy Development, Vietnam National University, Vietnam
[3]Faculty of Water Resources, Hanoi University of Natural Resources and Environment, Vietnam

Correspondence: Louise Schreyers (louise.schreyers@wur.nl)

Abstract. Plastic is an emerging pollutant, and the quantities in rivers and oceans are expected to increase. Rivers are assumed to transport land-based plastic into the ocean, and the fluvial and marine transport processes have been relatively well studied to date. However, the processes controlling the transport in tidal rivers and estuaries, the interface between fluvial and marine systems, remain largely unresolved. For this reason, current estimates of riverine plastic pollution and export into the ocean remain highly uncertain. Hydrodynamics in tidal rivers and estuaries are influenced by tides and freshwater discharge. As a consequence, flow velocity direction and magnitude can change diurnally. In turn, this impacts the transport dynamics of solutes and pollutants, including plastics. Plastic transport dynamics in tidal rivers and estuaries remain understudied, yet the available observations suggest that plastics can be retained here for long time periods, especially during periods of low net discharge. Additional factors such as riparian vegetation and riverbank characteristics, in combination with bidirectional flows and varying water levels, can lead to even higher likelihood of long-term retention. Here, we provide a first observation-based estimate of net plastic transport on a daily time scale in tidal rivers. For this purpose, we developed a simple Eulerian approach using sub-hourly observations of plastic transport and discharge during full tidal cycles. We applied our method to the highly polluted Saigon river, Vietnam, throughout six full tidal cycles in May 2022. We show that the net plastic transport is about 27-32% of the total plastic transport. We found that plastic transport and river discharge are positively and significantly correlated (Pearson's r = 0.87, R^2 = 0.75). The net transport of plastic is higher than the net discharge (27-32% and 18%, respectively), suggesting that plastic transport is governed by other factors than water flow. Such factors include wind, varying plastic concentrations in the water, and entrapment of plastics downstream of the measurement site. The plastic net transport rates alternate between positive (seaward) net transport and negative (landward) net transport, as a result of the diurnal inequality in the tidal cycles. We found that soft and neutrally buoyant items had considerably lower net transport rates than rigid and highly buoyant items (11-17% vs 31-39%), suggesting the retention time strongly depends on item characteristics. Our results demonstrate the crucial role of tidal dynamics and bidirectional flows in net plastic transport. With this paper we emphasize the importance of understanding fundamental transport dynamics in tidal rivers and estuaries to ultimately reduce the uncertainties of plastic emission estimates into the ocean.

https://doi.org/10.5194/egusphere-2022-1495
Preprint. Discussion started: 1 March 2023

1 Introduction

Exposure of terrestrial and aquatic ecosystems to plastic has gained considerable interest among the public and scientific community, due to its potential negative effects on the environment (Rochman et al., 2016). While the environmental risks posed by plastics remain to date largely uncertain, its presence in the environment is widely perceived as undesirable from an economic, aesthetic and ethical perspective (Borrelle et al., 2017; Koelmans et al., 2021; Beaumont et al., 2019). Effective and timely reduction strategies require understanding of the transfer dynamics of plastics across ecosystems and within environmental compartments (van Emmerik and Schwarz, 2020). Rivers are one of the main pathways of plastics from land to the sea (Meijer et al., 2021). Recently, efforts have been made to use concepts from hydraulics, hydrology, fluvial geomorphology, sedimentology, and debris transport to resolve the open questions of river plastic transport (Liro et al., 2020; Valero et al., 2022; Waldschläger et al., 2022). In particular, river plastic transport processes have been increasingly investigated in recent years in relation to hydrology. Observational studies have demonstrated the strong response of plastic transport to high river discharge events (van Emmerik et al., 2022a, b). Extreme discharge events such as floods mobilize large quantities of plastic and can lead to increased plastic emissions into the ocean (Roebroek et al., 2021a; van Emmerik et al., 2022b; Hurley et al., 2018). Under normal hydrological conditions, the relation between plastic transport and discharge varies between catchments and is non-trivial (Roebroek et al., 2022; van Emmerik et al., 2022a). Despite growing efforts to link plastic transport to hydrological processes, the transfer dynamics from rivers to sea remain poorly understood (van Emmerik et al., 2022c). Ultimately, the transfer processes in the lower reaches of rivers - in tidal rivers and estuaries - are the most crucial aspect for quantifying plastic emissions into the ocean. Yet, these plastic transfer processes at the river-ocean interface are arguably the most understudied aspect of riverine plastic transport.

Tidal rivers and estuaries are key components of river systems, as they form the interface between rivers and coastal environments (Hoitink and Jay, 2016). In tidal rivers, flows are affected by the combination of freshwater discharge and coastal forcing processes, such as tides. The interactions between river discharge and tidal dynamics ultimately affects the water, sediment and pollutant budgets (Healy et al., 2007; Tessler et al., 2018; Fernandes and Pillay, 2010). This can result in either net export towards the coastal water or net import landward, depending on the spatio-temporal scales considered. For example, characterizing net sediment transport requires quantifying the balance between landward supply and retention mechanisms within the estuarine zone. Various pollutants are similarly affected by bidirectional flows, with both net export and import being observed depending on the tidal dynamics (Fernandes and Pillay, 2010).

Several plastic research studies have aimed to quantify global riverine emissions of plastic into the sea (Jambeck et al., 2015; Lebreton et al., 2017; Schmidt et al., 2017; Meijer et al., 2021). River transport models typically include freshwater discharge as a determining variable for the total export into the sea, but do not consider tidal effects on net water discharge (Lebreton et al., 2017; Schmidt et al., 2017; Meijer et al., 2021). To date, no plastic transport model accounts for the influence of tidal dynamics on plastic emissions into the sea. Meijer et al. (2021) postulated that the probability that riverine plastic reaching the ocean increase with proximity to the river mouth, because larger cross-sectional areas in downstream reaches will reduce the likelihood of plastic trapping along riverbanks. We argue that in tidal rivers and estuaries, bidirectional flows and

https://doi.org/10.5194/egusphere-2022-1495
Preprint. Discussion started: 1 March 2023

other processes including turbulent mixing, entrapment in mudflats and vegetation could generate the opposite effect. With increasing tidal influence towards the river mouth, higher retention times of plastic within the system can be expected. This can ultimately result in lower plastic net transport rates downstream than upstream of the river system. Overall, current literature assumes that river plastic emissions are equivalent to plastic transport estimated most downstream (Meijer et al., 2021). This neglects retention dynamics within tidal rivers and estuaries, as well as potential landward transport. Acha et al. (2003) found that salinity fronts in estuaries act as a physical barrier that accumulates plastic. More recent studies have also shown the limited nature of plastic export in estuaries (Fernandino et al., 2016; A.G.López et al., 2020; Ledieu et al., 2022; Sutton et al.; Tramoy et al., 2020b, a). For instance, A.G.López et al. (2020) simulated plastic transport in the Chesapeake estuary (USA) and found that only 5% of the annual microplastic transport was exported into coastal waters, whereas the overwhelming majority (94%) beached on the estuarine shores.

Both Eulerian and Lagrangian-based approaches have been used to study solutes transfer dynamics from rivers to the ocean, notably in the field of sediment transport (Ballio et al., 2018). Lagrangian approaches follow the motion of particles, whereas Eulerian approaches describe the motion of particles over a spatially fixed volume. Most observation-based studies on plastic transport in tidal rivers and estuaries follow a Lagrangian approach, in that they study the transport and accumulation dynamics of a finite number of items Ledieu et al. (2022); Ryan and Perold (2021); Sutton et al.; Tramoy et al. (2020a, b). These studies all show that plastic trajectories are affected by both non-uniform advection (longitudinal) and diffusive (multi-directional) transfer processes. Mobile plastics travel limited distances, although a considerable share of plastics will deposit in various riverine compartments and be retained for years to decades (Tramoy et al., 2020b, a). Such transfer dynamics are the result of both limited transport caused by bidirectional flows and (temporary) trapping in vegetation and along riverbanks. Despite the growing evidence that tidal and estuarine dynamics attenuate plastic emissions into the oceans, net plastic transport has never been measured during full tidal cycles. The difficulty in conducting measurements at night (due to the lack of daylight) and the resource intensive nature of continuous measurements likely explain why such measurements have not been done thus far.

For this study, we developed a simple and easily transferable approach to quantify net plastic transport over tidal cycles at a river cross-section, in relation to total plastic transport. By using a Eulerian approach, we considered a fixed spatial domain in which we estimated plastic transport. This approach entails measuring plastic transport and water flow dynamics (river discharge, flow velocity and water levels) at a sub-hourly frequency. We applied this method to the Saigon river, Vietnam, in May 2022, and estimated net and total plastic transport over six full tidal cycles. For the first time, we were able to estimate net plastic transport in a tidal river, based upon field observations and using an Eulerian approach. We collected data on floating plastic transport for various plastic types and measured river discharge at a sub-hourly frequency. In this paper we demonstrate the limited net transport of plastic due to the tidal effects and how it varies by plastic type and by tidal cycle. With this paper we aim to highlight the crucial role of tidal rivers in the transport of riverine plastic into the ocean.

https://doi.org/10.5194/egusphere-2022-1495
Preprint. Discussion started: 1 March 2023

2 Methods

2.1 Study site

The field measurements were conducted at one site on the Saigon river (Vietnam), in Ho Chi Minh City (HCMC), at 70 km from the river mouth (Fig.1). The Saigon river originates in Cambodia, passes through the Dau Tieng reservoir, then progresses through a diverse agricultural and industrial region and then crosses HCMC, with a population of 9 million Vietnam's largest city. Approximately 20 km south of HCMC, the Saigon river meets the Dong Nai river where it forms the Nha Be river. The latter passes through the Can Gio Mangrove forest where it branches in multiple channels and then debouches in the East Sea (Nguyen et al., 2020) (Fig.1A). The Saigon river is affected by an asymmetric semi-diurnal tidal regime, usually resulting in a reversal of the flow direction twice a day. Tidal dynamics are registered up to the Dau Tieng reservoir, 140 km from the river month (Nguyen et al., 2021), and regulates net discharge in the Saigon river (Camenen et al., 2021). In addition, river discharge in the Saigon river is affected by both a strong seasonality between the wet and the dry seasons, with monthly mean net discharge varying between -80 and 320 $m^3 s^{-1}$ (Camenen et al., 2021).

2.2 Measurement setup

This study focuses on the transport of floating macroplastics larger than 0.5 cm, hereafter referred to as plastic. We measured plastic transport, water depth, and flow velocity at the Thu Thiem bridge (10.785984, 106.718332), located in the southern part of HCMC. The field measurements were conducted continuously over 74 hours and 30 minutes, from 1 to 4 May, 2022. Five observation points were monitored across the river width, to account for the spatial variability at the river cross-section in plastic transport, water depth, and flow velocity (Fig.1B). The observation points were chosen in order to maximize coverage of the entire river cross-section on the one hand and to minimize the influence of the bridge piers. Measurements were conducted on both sides of the bridge: during flood flow, the measurements took place on the northern side of the bridge, while the southern side was used during ebb flow. This allowed surveyors to face the flow direction during measurements and facilitated the handling of equipment in and out of the water. The bridge is approximately 14 m above the average water depth during measurements.

At each measurement location three instantaneous measurements were taken: floating plastic transport (section 2.3), the water depth (section 2.4), and the flow velocity (section 2.5). A minimum of two surveyors were present to conduct the instantaneous measurements. This was necessary during peak plastic transport periods, when values up to over 100 items min^{-1} were registered. In such cases, one surveyor conducted the visual counting while another noted down the values. Up to four surveyors could be present for instantaneous measurements, depending on availability. Each measurement round lasted on average 9 minutes. The measurement duration varied between 3 to 42 minutes, depending on the number of available surveyors, the presence of boat traffic which could further delay the measurement, and potential challenges with handling equipment. Measurements were conducted both during the day and at night. At night, a flashlight lamp (P18R Signature, Ledlenser, Germany, https://ledlenser.com/en/) was used to illuminate the water surface, estimate plastic transport and take equipment in and out of the water safely. The model used had 4500 lumen luminous flux.

https://doi.org/10.5194/egusphere-2022-1495
Preprint. Discussion started: 1 March 2023

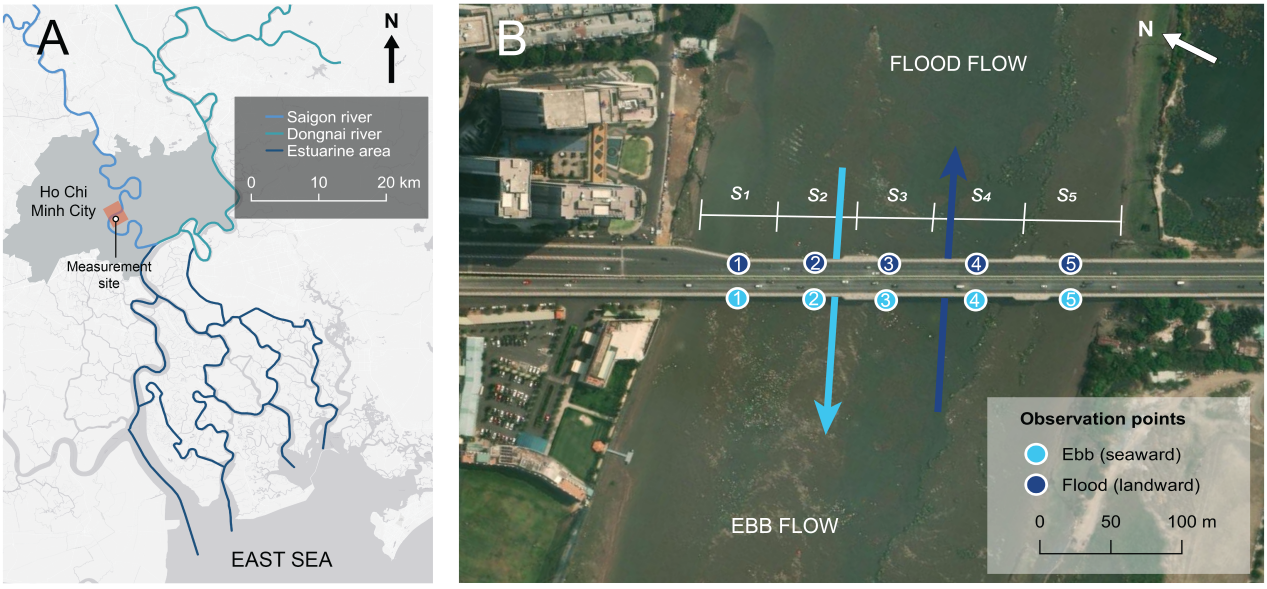

Figure 1. A. Measurement site within the Saigon - Dong Nai river system. B. Measurement site (Thu Thiem bridge, 10.785984, 106.718332) and locations. s_1, s_2, ... indicate the segment corresponding to each observation point. Copyright: © Bing Maps. Note the different north orientation for the two panels

2.3 Plastic transport estimates

Plastic transport was estimated using the visual counting method, developed by González-Fernández and Hanke (2017). All visible (> 0.5 cm) anthropogenic litter items floating at the water surface were counted for a duration of 2 minutes and classified according to various type of materials. The following eight categories were used: EPS (expanded polystyrene), PO_{hard} (hard polyolefins), PO_{soft} (soft polyolefins), PS (polystyrene), PET (polyethylene terephthalate), Multilayer plastics, Other plastic items and Other litter items (non-plastic). These plastic categories have been used in previous studies (van Emmerik et al., 2022a; Schreyers et al., 2021) and are considered suitable for a first-order identification of plastic types. In this study, we only consider plastic items and therefore do not report litter transport estimates. Plastic transport F [items h^{-1}] was calculated using the following equation (van Emmerik et al., 2022a):

$$F = \sum_{i=1}^{5} \frac{\overline{f_i}}{w_i} \frac{W}{5} \tag{1}$$

With mean plastic transport observation $\overline{f}$ [items h^{-1}] for observation point i at 5 observation points, observation track width w_i [m] and total river width W [m]. We considered an observation track width of 15 m, and a total river width of 298 m.

Plastic transport is often expressed in terms of mass transport in current literature (Lebreton et al., 2017; Meijer et al., 2021; Schmidt et al., 2017; van Emmerik et al., 2022a). Therefore, we also expressed plastic transport M in terms of mass transport

https://doi.org/10.5194/egusphere-2022-1495
Preprint. Discussion started: 1 March 2023

[kg day^{-1}], using the following equation (Vriend et al., 2020):

$$M = F \cdot \overline{m} \cdot c \tag{2}$$

With $\overline{m}$ expressing either the mean and median mass per plastic item [g] and c the conversion factor from g hour^{-1} to kg day^{-1}.

We used the mass statistics from van Emmerik et al. (2019). In this study, 3,022 items collected over 45 days at the same measurement location in the Saigon river were weighted and categorized into the following plastic type categories: EPS, PS, PO_{hard}, PO_{soft} and PET. For the categories 'Multilayer' and 'Other plastic' from our observations, we used the mean and median mass found for all items (respectively 10 g and 4.3 g). Median and mean mass values per item category are reported in Table D2 (Appendix D).

2.4 Water depth, flow velocity measurements and discharge estimates

Water depth was measured using a single beam sonar with Compressed High Intensity Radiated Pulse (CHIRP) (Deeper Smart Sonar Chirp 2, Lithuania, https://deepersonar.com/). The sonar was lowered from the bridge into the water using a rope. Once the sonar reached the water surface, water depth values could be read on a previously paired mobile phone using the Deeper Smart Sonar mobile application. The sonar was lost on 4 May, 2022 around 03:00 A.M. due to collision with a container ship. As a result, water depths were not recorded for the last 13 hours of measurements.

Near-surface flow velocities were measured using a propeller flow meter (Flowatch, JDC, Switzerland, https://www.jdc.ch/). The flow meter was lowered from the bridge into the water, at approximately one meter of depth from the surface, using a cable. The surface velocities were converted to depth-average velocity by multiplying the surface velocity by a coefficient of 0.85, typically used in natural channels (Rantz). Flow velocities for flood water flows were recorded as negative values, and as positive values for ebb water flows.

The cross-sectional area was estimated for each observation point, as follows:

$$a_i = w_i \cdot d_i \tag{3}$$

With width w_i [m] and depth d_i [m] per segment s_i. There are five segments, with an observation point in the middle. The water depth was measured at each observation point i and was considered as the averaged depth per segment. We estimated water discharge [m^3 s^{-1}] at the river cross-section as follows:

$$Q = \sum_{j=1}^{5} a_i \cdot \overline{v_i} \tag{4}$$

With $\overline{v}$ the depth averaged flow velocity [m s^{-1}] at each measurement location i. Because of the lack of water depth observations during the last 13 hours of measurement, the resulting discharge estimates only covered 5 out of the 6 tidal cycles. This data gap was filled by estimating river discharge based on the significant and strong relation found with flow velocity for

https://doi.org/10.5194/egusphere-2022-1495
Preprint. Discussion started: 1 March 2023

all observed values (Pearson's r = 0.99, R^2 = 0.99, and p-value < 0.01) (Fig. A in Appendix A). The following equation was used to fill missing discharge estimates:

$$Q = \overline{v} \cdot 3393 \tag{5}$$

Because of the data gap in water depths, we prefer to report the relation between plastic transport and water flow based on flow velocity estimates (for instance for Fig.3 and 4), as there is less uncertainty on those values compared with river discharge estimates.

2.5 Temporal data harmonization

Plastic transport, water depths and flow velocities could not be measured at precisely regular time intervals, due to constraints in handling equipment, varying number of available surveyors and varying distances between measurement locations. For this reason, plastic transport, flow velocity and discharge values were interpolated to a regular time interval using two different methods. Flow velocity and discharge values were interpolated using tidal characteristics. Tidal constituents were analyzed using the Unified Tidal Analysis and Prediction (UTide) package in Python 3.4 (Codiga, 2011). This enabled us to determine the coefficients (phase and amplitude) for each tidal constituent, which were in turn used to interpolate our time-series. We present the results of the tidal constituent analysis in Appendix B, as they are not considered novel findings but were nonetheless crucial for flow velocity and discharge interpolation. The temporal interpolation was done to a 10-minute interval, because it is close to the time interval between observations (9 minutes on average). Plastic transport was also interpolated to 10-minute intervals, using a linear interpolation.

2.6 Calculating net and total plastic transport and discharge

Here we define ebb and flood as the tidal phases in which the water current is flowing seaward and landward, respectively. While usually seaward plastic transport dominates during the ebb phase and landward plastic transport during the flood phase, short lags in time (of about a few minutes) were noted during slack periods (Fig.2). For instance, although the overall river cross-section are dominated by one flow direction, reverse flow could still be (temporally) observed at one or a few measurement locations. If at those measurement locations plastic densities out-weights densities at the remaining measurement locations, a discrepancy can be noted at the cross-section between water flow and plastic transport directions.

Based on the distinction between flood and ebb phases, we calculated the net plastic transport during ebb and flood, flow velocities and river discharges. We introduce a relative measure of net transport, hereby called delivery ratio (d_r). Using a relative metric allows for easier comparison across various spatio-temporal scale and within systems with varying plastic pollution levels. The d_r expresses the ratio [%] between net and total transported volumes, as follows:

$$d_r = \frac{V_{ebb} - V_{flood}}{V_{ebb} + V_{flood}} \cdot 100\% \tag{6}$$

https://doi.org/10.5194/egusphere-2022-1495
Preprint. Discussion started: 1 March 2023

To this scope, we calculated the total transported volumes of plastic, flow velocity and discharge during ebb and flood, as follows:

$$V_{ebb} = \int_{T_{ebb}} y(t)dt \qquad \text{with v} > 0 \tag{7}$$

$$V_{flood} = \int_{T_{flood}} y(t)dt \qquad \text{with v} < 0 \tag{8}$$

T_{ebb} and T_{flood} indicate the ebb and flood tidal phase, respectively, y the values integrated over time t (plastic transport, flow velocity and discharge) and v the flow velocity. The integral values for flow velocity and discharge correspond respectively to the total river surface length [m] and river volume [m^3] that passed by the measurement location per tidal phase. The integral values for plastic transport corresponds to the total volume of plastic items passing by the measurement location. Figure 2 gives an example for the V_{ebb} and V_{flood} calculation, using the flow velocity as the variable of reference for distinguishing between flood and ebb.

We also determined the net plastic transport, flow velocity and discharge (f_{net}) in absolute values (respectively in items $hour^{-1}$, m s^{-1} and m^3 s^{-1}) as follows:

$$f_{net} = \frac{V_{ebb} + V_{flood}}{T_{ebb} + T_{flood}} \tag{9}$$

In addition, we calculated the mean plastic transport, flow velocity and discharge for each ebb and flood cycle (f_{ebb} and f_{flood}, respectively), as follows:

$$f_{ebb} = \frac{V_{ebb}}{T_{ebb}} \tag{10}$$

$$f_{flood} = \frac{V_{flood}}{T_{flood}} \tag{11}$$

https://doi.org/10.5194/egusphere-2022-1495
Preprint. Discussion started: 1 March 2023

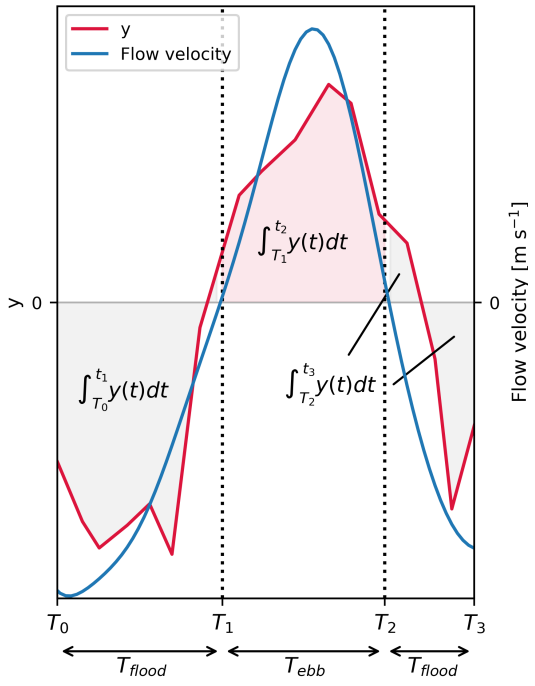

Figure 2. Example of calculation of integral areas for the ebb and flood phases of the tidal cycle. The grey shaded areas correspond to the integral during flood, the red shaded area to the integral during ebb. Y represents the variable to be integrated, which could be plastic transport, river discharge or flow velocity.

3 Results

3.1 Net plastic transport less than one-third of total plastic transport

Over the six tidal cycles considered, we found a seaward mean net transport of approximately $3.1 \cdot 10^3$ items hour^{-1}, corresponding to 400-760 plastic kg day^{-1} (Table 1). This represents only about 27-32% of total plastic transport. This ratio is lower for river discharge and flow velocity (18%) (Table 1). Overall, these findings suggest that although plastic transport is mainly governed by net discharge and flow velocity (R^2 = 0.75 between plastic transport and river discharge), other factors lead to higher net transport of plastics (see Discussion). The plastic mass transport estimates vary by a factor of almost two, depending on whether the mean or median mass of items is considered (Table 1). This does not significantly alter the delivery ratios found for plastic mass transport, which in agreement with the delivery ratio found for items transport (27% for mass transport based on the mean mass, 32% based on median mass and 27% for items transport).

https://doi.org/10.5194/egusphere-2022-1495
Preprint. Discussion started: 1 March 2023

Table 1. Summary statistics for plastic transport, flow velocity and discharge

	Ebb (f_{ebb})	**Flood** (f_{flood})	**Net** (f_{net})	**Delivery ratio** (d_r) **[%]**
Plastic items transport [items hour^{-1}]	$1.5 \cdot 10^4$	$-8.6 \cdot 10^3$	$3.1 \cdot 10^3$	27
Plastic mass transport (median mass) [kg day^{-1}]	$1.7 \cdot 10^3$	$-8.3 \cdot 10^2$	$4.0 \cdot 10^2$	32
Plastic mass transport (mean mass) [kg day^{-1}]	$3.6 \cdot 10^3$	$-2.0 \cdot 10^3$	$7.6 \cdot 10^2$	27
Flow velocity [m s^{-1}]	0.34	-0.23	0.051	18
River discharge [m^3 s^{-1}]	1100	-790	170	18

Water flow in the Saigon river follows a sinusoidal pattern, with clear alternations between ebb and flood phases determined by the tidal cycle and its various phases in rising and falling limbs and slack water periods (Fig. 3). The tidal variation in flow velocity shows positive residuals, with both higher peaks in flow velocity during the ebb than flood phase of the tidal cycles (maximum and minimum flow velocity: 0.56 and -0.41 m s^{-1}, respectively). The flood phase is longer than the ebb phase (38 hours and 20 minutes and 36 hours and 10 minutes, respectively). We found a seaward net discharge of 172 m^3 s^{-1} over the measurement period, corresponding to relative net water transport of approximately 18% of total water flow (Table 1). Plastic transport follows a similar asymmetrical sinusoidal pattern to flow velocity (Fig.3). Plastic transport was found to be highly positively correlated with river discharge and flow velocity (Pearson's r = 0.87, R^2 = 0.75, and p-value < 0.01 for plastic transport in relation to both discharge and flow velocity). Plastic transport can be expressed as a linear function in relation to discharge for all items aggregated (Appendix C, Fig. C1), as well as by plastic types (Appendix C, Fig. C2). For the latter, the R^2 values could indicate the degree to which river discharge influences the transport of these different plastic types. With this assumption, transport of PS and PO$_{soft}$ items are the most linearly influenced by river discharge (R^2 of respectively 0.71 and 0.68). It is likely, however, that the lower R^2 values are also an indicator of the stochastic component of plastic concentrations in the river system.

Despite the strong and significant correlation found between river discharge and plastic transport, similar discharge values were observed for a wide range of plastic transport. For instance, for peak discharges of over 2,000 m^{3}s^{-1}, plastic transport varied by a factor of almost four, between 0.72-2.8 $\cdot$ 10^4 items hour^{-1} (Appendix C, Fig. C1). We hypothesize that varying contributions of different plastic types to the overall plastic transport explain this discrepancy. In particular, a higher share of EPS and PO$_{soft}$, two types of items for which the relation between transport and river discharge is characterized by a steeper slope (Appendix C, Fig. C2), might lead to higher transport during peak discharge periods. This hypothesis seems to be confirmed by our observations (Appendix C, Fig. C1), with EPS and PO$_{soft}$ items making up for more than 80% of the plastic composition during peak plastic transport, much higher than on average (56%) (Appendix C, Fig. C1). In addition, a hysteresis pattern is noticeable between plastic transport and river discharges, but was not found to be consistent between rising and falling limbs of the tidal cycle, for both the entire time-series and across the different tidal cycles observed (Appendix C, Fig. C1 and C3). Overall, estimating plastic transport based on a simple linear model from measured discharge would yield

https://doi.org/10.5194/egusphere-2022-1495
Preprint. Discussion started: 1 March 2023

large uncertainties, especially for peak transport values. There is no clear explanation for the wide range of plastic transport values during peak discharge events. The observed hysteresis pattern could be related to the asymmetry in rising and falling limb and/or from other sources of uncertainties, including varying concentrations of different plastic types.

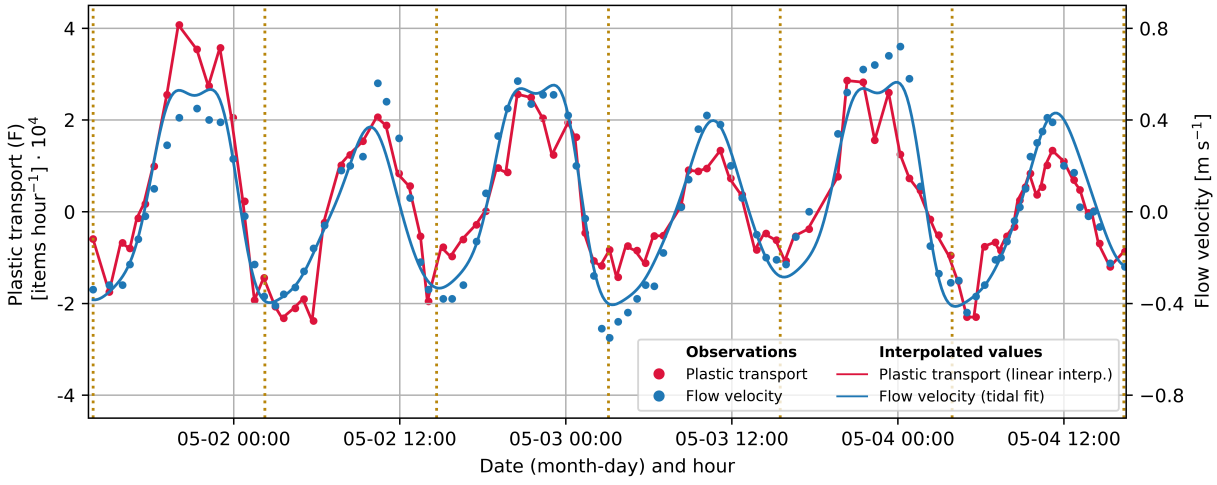

Figure 3. Plastic transport and flow velocity over the entire measurement period. The dotted yellow lines separate each tidal cycle.

3.2 Diurnal inequality results in alternating positive and negative delivery ratios

During the measurement period, water flow exhibits a mixed tidal cycle (i.e. two high and low tides each lunar day), resulting in diurnal inequality and an alternation between ebb and flood dominated tidal cycles. The first, third and fifth tidal cycles are ebb dominated, as the total volume of water is larger during the ebb phase of the cycle than during the flood phase ($V_{ebb} > V_{flood}$ for river discharge values). The second, fourth and sixth tidal cycle exhibit, on the contrary, flood dominance $V_{flood} > V_{ebb}$ for river discharge values).

Because of this diurnal alternation, we could therefore expect varying net discharge and plastic transport rates depending on whether the tidal cycle was ebb or flood dominated. We found positive net plastic transport, flow velocity and discharge, for ebb dominated cycles (1,3 and 5), for both mean values and delivery ratios (Table 2). Negative net plastic transport, flow velocity and river discharge were measured for flood dominated cycles (2, 4 and 6). This indicates that diurnal variations in tidal dynamics and freshwater discharge, resulting in asymmetry in peaks, are an important component in explaining the variability in net flow and transport. In line with this, the tidal constituent analysis showed that the main daily tidal component (K1) is the second most important tidal component of our time-series (Appendix B, Tidal constituent analysis). As a result of the alternation between ebb and flood dominated cycles, the tidal cycle averaged net transport rates varied by a factor of nearly -4 between cycles ($1.1 \cdot 10^4$ items hour^{-1} for the first cycle and $-2.8 \cdot 10^3$ items hour^{-1} for the sixth cycle).

https://doi.org/10.5194/egusphere-2022-1495
Preprint. Discussion started: 1 March 2023

We hypothesize that high plastic delivery ratios could be governed by either averaged-cycle high net river discharge, high plastic concentrations in the water or a combination of both. For the first tidal cycle, the high plastic delivery ratio (58-63%) seems to be mainly driven by high plastic concentrations, as the flow velocity and river discharge delivery ratio is not particularly high (33%). The highest mean plastic transport during the ebb phase was found for this cycle ($2.6 \cdot 10^4$ items hour^{-1}), almost 3.5 times more than for the entire measurement period) (Appendix D, Table D1). For the third tidal cycle, the plastic delivery ratio was closer to the flow velocity and river discharge delivery ratio (50-51% and 41%, respectively), and the net river discharge was found to be quite high (470 m^3 s^{-1}); more than 20% higher in fact than on the first cycle (380 m^3 s^{-1}). This suggests that the high delivery ratio of plastic transport found for the third tidal cycle was mainly governed by high net discharge. The highest plastic delivery ratio was registered during the fifth tidal cycle (66-69%). Net river discharge was also at its highest during this tidal cycle (520 m^3.s^{-1}) and net plastic transport was double than average ($7.7 \cdot 10^3$ items hour^{-1} for the fifth tidal cycle and $3.1 \cdot 10^3$ items hour^{-1} on average for the entire measurement period), but lower than during the first tidal cycle ($1.1 \cdot 10^4$ items hour^{-1}). During the fifth tidal cycle, a combination of high net discharge and high plastic concentrations likely explains the high plastic delivery ratio found.

Overall, plastic delivery ratios calculated based on items transport and mass transport are in good agreement, with no more than $\pm$5% of difference between the three values. One notable exception was found for the second tidal cycle, during which the delivery ratio of plastic mass transport, based on the median mass of items, is considerably higher than both the mass transport based on mean mass of items, and the items transport (-1% compared to -11% and -15%, respectively). The mean mass per item is very similar among items compared to the mean mass of all items: with the exception of PET (mean mass: 20 g) all items have a mass comprised between 7.0 and 12 g, with an overall average of 10 g per item. The median mass is more variable among items, ranging between 1.9 and 7.7 g (with the exception of PET, median mass = 21 g) (Table C2). As a result, peaks in transport of items heavier or lighter than others can alter the averaged cycle net transport rates. Anticipating on section 3.3, the peak in polystyrene items (PS) observed during the ebb phase of the tidal cycle, can explain the lower delivery ratio registered for the median mass transport. Indeed, the median mass for PS items is higher than the averaged median mass for all items (6.0 g vs 4.3 g, 33% difference), whereas this difference is less pronounced for the mean mass (11 g vs 10 g, difference of less than 10%).

https://doi.org/10.5194/egusphere-2022-1495
Preprint. Discussion started: 1 March 2023

Table 2. Net plastic transport, flow velocity and river discharge and associated delivery ratios by tidal cycle. Each tidal cycle lasts 12 hours 25 minutes

	Cycle	1	2	3	4	5	6
Items transport	Net (f_{net}) [items hour^{-1}]	$1.1 \cdot 10^4$	$-1.9 \cdot 10^3$	$6.1 \cdot 10^3$	$-1.0 \cdot 10^3$	$7.7 \cdot 10^3$	$-2.9 \cdot 10^3$
	Delivery ratio (d_r) [%]	58	-15	51	-14	69	-33
Mass transport (median mass)	Net (f_{net}) [kg day^{-1}]	$1.4 \cdot 10^3$	$-1.7 \cdot 10^1$	$6.0 \cdot 10^2$	$-6.4 \cdot 10^1$	$7.9 \cdot 10^2$	$-2.3 \cdot 10^2$
	Delivery ratio (d_r) [%]	63	-1	51	-8	64	-26
Mass transport (mean mass)	Net (f_{net}) [kg day^{-1}]	$2.6 \cdot 10^3$	$-3.4 \cdot 10^2$	$1.4 \cdot 10^3$	$-2.3 \cdot 10^2$	$1.7 \cdot 10^3$	$-6.3 \cdot 10^2$
	Delivery ratio (d_r) [%]	58	-11	50	-13	66	-31
Flow velocity	Net (f_{net}) [m s^{-1}]	0.11	-0.056	0.14	-0.034	0.15	-0.0075
	Delivery ratio (d_r) [%]	33	-24	41	-14	46	-3
River discharge	Net (f_{net}) [m^3 s^{-1}]	380	-190	470	-120	520	-30
	Delivery ratio (d_r) [%]	33	-24	41	-14	46	-3

3.3 Net plastic transport varies with plastic type

We determined the transport and delivery ratio per plastic type (Fig. 4). Plastic items differ in their shape, size, buoyancy and rigidity, characteristics that could influence their transport processes. We found that the amplitude in plastic transport varies significantly depending on both the tidal cycle and the type of items considered. Net transport vary by two orders of magnitude depending on the plastic type considered (from $1.5 \cdot 10^3$ for EPS items to $-3.6 \cdot 10^1$ items hour^{-1} for Other plastic items) (Table 3). We calculated a positive net transport in relation to total transport ($d_r > 0$) for all plastic types, with the exception of PO$_{hard}$ and Other plastic. These two categories correspond to the least commonly found items (respectively 3 and 2% of the total plastic items). The delivery ratio varied between 62% and -15% depending on the plastic type. Large items such as PET (e.g.: plastic bottles) and rigid and highly buoyant items such as EPS (e.g.: expanded polystyrene such as foam) and PS (polystyrene, such as plates) registered the highest net export (62%, 39% and 31%, respectively). On the contrary, soft and neutrally buoyant items such as PO$_{soft}$ (e.g.: bags and foils) and Multilayer (food packaging) had lower net transport rates (17% and 11%, respectively).

Moreover, large fluctuations in plastic transport were noted depending on the tidal cycle. For instance, transport in EPS, PO$_{soft}$ and PS are particularly high during the first tidal cycle during its ebb phase. Transport of Multilayer items is high during the second tidal cycle, similarly to transport of PS items, also during the ebb phase. Our results suggest that the relative contribution of item types is highly variable, with varying concentrations per plastic type at the water surface, probably resulting from varying inputs of plastics into the river.

https://doi.org/10.5194/egusphere-2022-1495
Preprint. Discussion started: 1 March 2023

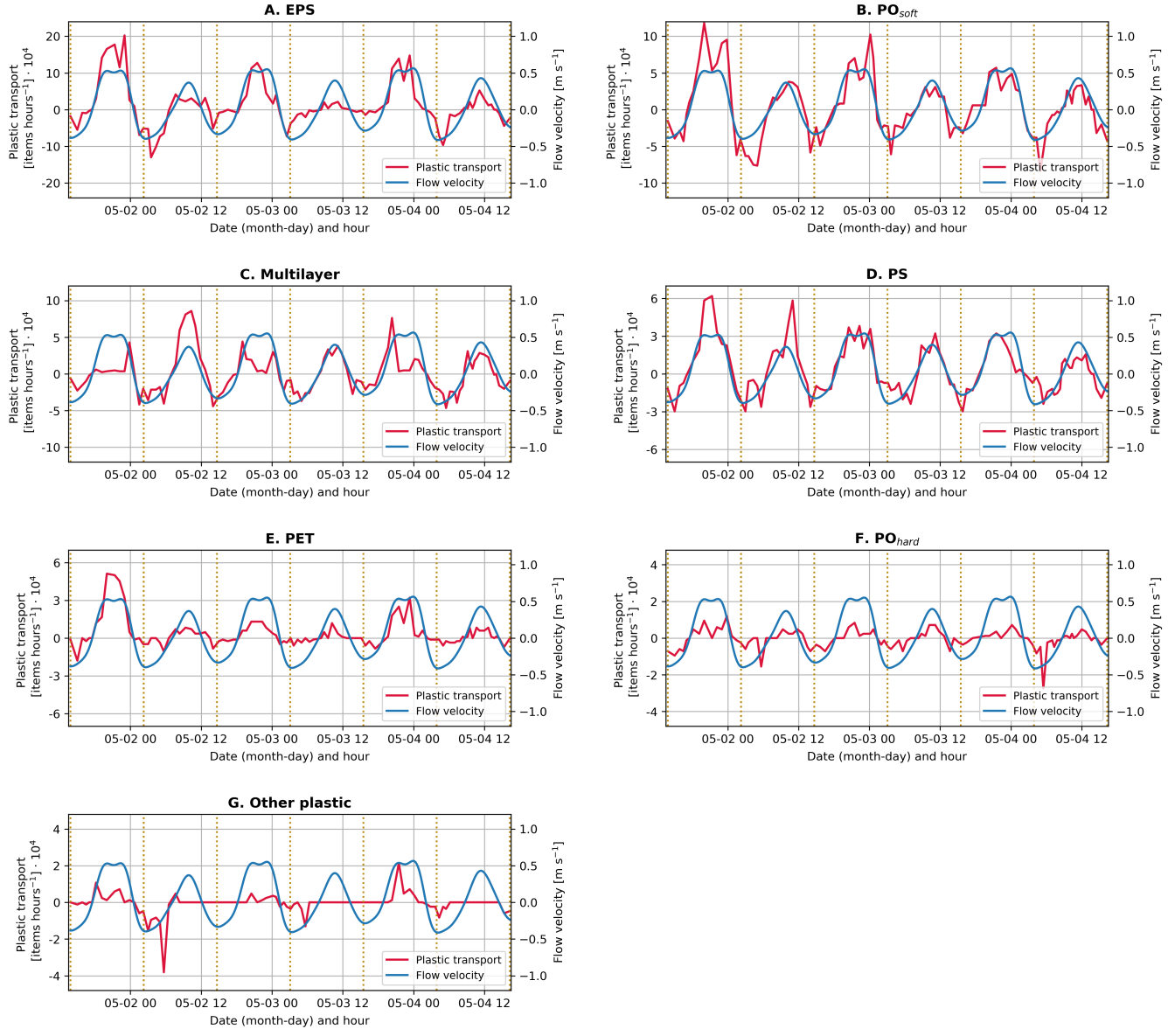

Figure 4. Plastic transport by category type and flow velocity over the entire measurement period (A-G). The dotted yellow lines separate each tidal cycle. The y-axis differ depending on the subplot for plastic transport, to better visualize the value distributions. Items are ranked from the most frequently found on average (EPS) to the least frequently found on average (Other plastic)

https://doi.org/10.5194/egusphere-2022-1495
Preprint. Discussion started: 1 March 2023

Table 3. Summary statistics for plastic transport, flow velocity and discharge by material type. The discrepancy in sign for certain values between net transport and delivery ratios is due to the fact that the latter was calculated based on the integral values for input and output phases, whereas net transport resulted from the difference between mean output and input transport.

Plastic type	Variables	Ebb (f_{ebb})	Flood (f_{flood})	Net (f_{net})	Delivery ratio (d_r) [%]
EPS	Items transport [items hour^{-1}]	$5.4 \cdot 10^3$	$-2.4 \cdot 10^3$	$1.5 \cdot 10^3$	39
	Mass transport (median mass) [kg day^{-1}]	$2.5 \cdot 10^2$	$-1.1 \cdot 10^2$	$7.0 \cdot 10^1$	
	Mass transport (mean mass) [kg day^{-1}]	$9.1 \cdot 10^2$	$-4.0 \cdot 10^2$	$2.5 \cdot 10^2$	
PO$_{soft}$	Items transport [items hour^{-1}]	$3.7 \cdot 10^3$	$-2.6 \cdot 10^3$	$5.4 \cdot 10^2$	17
	Mass transport (median mass) [kg day^{-1}]	$2.6 \cdot 10^2$	$-1.8 \cdot 10^2$	$3.8 \cdot 10^1$	
	Mass transport (mean mass) [kg day^{-1}]	$9.3 \cdot 10^2$	$-6.5 \cdot 10^2$	$1.4 \cdot 10^2$	
Multilayer	Items transport [items hour^{-1}]	$2.1 \cdot 10^3$	$-1.7 \cdot 10^3$	$2.1 \cdot 10^2$	11
	Mass transport (median mass) [kg day^{-1}]	$2.2 \cdot 10^2$	$-1.7 \cdot 10^2$	$2.1 \cdot 10^1$	
	Mass transport (mean mass) [kg day^{-1}]	$5.2 \cdot 10^2$	$-4.1 \cdot 10^2$	$5.0 \cdot 10^1$	
PS	Items transport [items hour^{-1}]	$2.1 \cdot 10^3$	$-1.1 \cdot 10^3$	$4.9 \cdot 10^2$	31
	Mass transport (median mass) [kg day^{-1}]	$3.0 \cdot 10^2$	$-1.6 \cdot 10^2$	$7.0 \cdot 10^1$	
	Mass transport (mean mass) [kg day^{-1}]	$5.3 \cdot 10^2$	$-2.8 \cdot 10^2$	$1.2 \cdot 10^2$	
PET	Items transport [items hour^{-1}]	$1.1 \cdot 10^3$	$-2.5 \cdot 10^2$	$4.2 \cdot 10^2$	62
	Mass transport (median mass) [kg day^{-1}]	$5.5 \cdot 10^2$	$-1.3 \cdot 10^2$	$2.1 \cdot 10^2$	
	Mass transport (mean mass) [kg day^{-1}]	$5.3 \cdot 10^2$	$-1.2 \cdot 10^2$	$2.0 \cdot 10^2$	
PO$_{hard}$	Items transport [items hour^{-1}]	$3.0 \cdot 10^2$	$-3.3 \cdot 10^2$	$-1.7 \cdot 10^1$	-5
	Mass transport (median mass) [kg day^{-1}]	$5.5 \cdot 10^1$	$-6.1 \cdot 10^1$	$-3.1 \cdot 10^0$	
	Mass transport (mean mass) [kg day^{-1}]	$8.8 \cdot 10^1$	$-9.7 \cdot 10^1$	$-5.0 \cdot 10^0$	
Other plastic	Items transport [items hour^{-1}]	$2.1 \cdot 10^2$	$-2.8 \cdot 10^2$	$-3.6 \cdot 10^1$	-15
	Mass transport (median mass) [kg day^{-1}]	$2.1 \cdot 10^1$	$-2.9 \cdot 10^1$	$-3.8 \cdot 10^0$	
	Mass transport (mean mass) [kg day^{-1}]	$4.9 \cdot 10^1$	$-6.7 \cdot 10^1$	$-8.8 \cdot 10^0$	

4 Discussion

4.1 Limited net plastic transport in tidal rivers

With this study, we demonstrated that tidal dynamics can strongly limit plastic transport in downstream direction. We found that net plastic transport corresponds to less than 30% of the total transport, as a result of bidirectional flows and semi-diurnal and diurnal tidal dynamics. These findings are in line with other studies that demonstrated that plastic is transported over shorter distances in estuaries compared to the freshwater reaches of rivers (Ledieu et al., 2022; Tramoy et al., 2020a, b). Due to limited export out of the system, plastics can be retained over long periods of time, in certain cases surpassing decades as shown for the Seine river (France) (Tramoy et al., 2020b) . Long retention times likely lead to high plastic concentrations, if we consider the additional inputs of plastic into the water. In the Saigon river, a clear seasonality in net discharge is observed. Peak net discharge (typically exceeding 200 m^3 s^{-1}) only occur for a couple of months, usually between the months of June and August (Camenen et al., 2021). Plastic concentrations likely only decrease significantly during these high discharge periods, due to an increase in net plastic transport and export. In this study, we only considered macroplastic (> 0.5 cm), but long macroplastic residence times would likely impact microplastic concentrations as well. Increased plastic break-down and degradation due to

https://doi.org/10.5194/egusphere-2022-1495
Preprint. Discussion started: 1 March 2023

a long presence of macroplastics in the river system probably leads to increased microplastic concentrations as well (Delorme et al., 2010; Lahens et al., 2018).

To date, global river plastic transport and emission models do not consider tidal influence, which likely results in an overestimation of global plastic emissions into the oceans. Models that use discharge as a predictor for riverine plastic transport should be considered as export models from the non-tidal part of the river to its tidal zone, but not yet into the ocean. We found that plastic transport was strongly correlated to instantaneous discharge, which could be then used to estimate net discharge and net plastic transport. Thus, estimating transport and emission in the tidal zone could rely on measured instantaneous discharge, instead of only using freshwater discharge estimates. Using rainfall-runoff models to estimate freshwater discharge rates entirely neglects tidal influence on net plastic transport and emissions into the ocean. Such approaches however have been used broadly to estimate global plastic emissions (Lebreton et al., 2017; Meijer et al., 2021). Measuring discharge in tidal systems however remains very challenging and as a result, most gauging stations are located upstream of the tidal region (Gisen and Savenije, 2015; Nguyen and Nguyen, 2018). Furthermore, considering measured discharge as a more reliable predictor for plastic transport in tidal rivers remains problematic. Establishing a fixed relation between river discharge (and other environmental drivers) and plastic transport is ultimately challenging because it cannot take into account temporal variations in plastic concentrations in the water, due to human behaviors (littering and cleaning) (Roebroek et al., 2021b). By drawing an analogy with sediment rating curves, we can hypothesize that the rating parameters indicating availability and concentrations of plastics probably change more rapidly compared to sediment supply. The time-scales governing variability in plastic inputs into the water are likely to be shorter compared to those of sediment loads. In line with this hypothesis, Tasseron et al. (3001under review) observed large temporal (daily and monthly) fluctuations in plastic transport in urban waterways, a likely result of higher inputs of plastics during peak hours and seasons of outdoor human activity. The inherent difficulties in obtaining discharge estimates for tidal regions worldwide on the one hand and the limitations of using discharge as a reliable predictor of plastic transport, on the other hand, call for alternative approaches in estimating plastic emissions. Probabilistic methods that introduce a corrective factor for decreasing downstream plastic transport with decreasing distance to the river mouth could improve global transport estimates.

4.2 River plastic transport is highly variable depending on the tidal dynamics

In addition to the limited downstream transport of plastic, our analysis showed that plastic transport rates are highly variable in time. This temporal variability in plastic transport rates is two-fold: (i) between peak and averaged semidiurnal net transport rates, and (ii) between the different averaged semidiurnal net transport rates. Peak transport values ranged from -2.4 $\cdot$ 10^4 and 4.1 $\cdot$ 10^4 items hour^{-1} over the studied period. As a consequence, field measurements that would be undertaken at the peak of either the flood and ebb flow of the tide or during a slack water phase would likely result in an overestimation or underestimation of net plastic transport. For instance, the highest mean plastic transport found during the ebb and flood phases (2.6 $\cdot$ 10^4 and -1.2 $\cdot$ 10^4 items hour^{-1}, respectively) are approximately one order of magnitude higher than the mean net plastic transport (3.1 $\cdot$ 10^3 items hour^{-1}) for the entire measurement period. Similarly, studies on sediment transport in tidal rivers found that instantaneous peak transport values are at least one order of magnitude higher than the net (residual) sediment

https://doi.org/10.5194/egusphere-2022-1495
Preprint. Discussion started: 1 March 2023

transport (Gatto et al., 2017). The large discrepancy between instantaneous and net plastic transport highlights the need to estimate transport rates based on longer observation periods than usually done in current riverine transport studies. For example, González-Fernández et al. (2021) quantified plastic transport over 42 rivers, over 410 hours of measurement, amounting to only 25 minutes of observation per river. Furthermore, we showed that net estimates of plastic transport vary greatly depending on whether measurements are conducted during an ebb or flood dominated cycles, resulting in either positive (seaward) or negative (landward) net plastic transport, and values ranging by a factor of nearly -4 between the highest and lowest net transport per cycle. Overall, the high variability between peak and averaged cycle net plastic transport, coupled with the variability within net plastic transport per tidal cycle highlight both the uncertainty in quantifying net plastic transport and the dependency on the temporal scale considered.

This study was the first to quantify plastic transport during full tidal cycles using a Eulerian approach. We only considered short-term tidal dynamics, namely the alternation between flood and ebb tidal phases and the diurnal cycles. Longer-term patterns, such as the cycle in neap and spring tides, the seasonality in net discharge or peaks in freshwater discharge could all influence flow dynamics and thus significantly alter plastic transport processes. Fernandino et al. (2016) for instance observed higher floating litter densities during the spring ebb tides. This suggests that co-occurrences in hydrological conditions are also of interest to understand long-term plastic transport dynamics in tidal rivers. Additional measurements of plastic transport throughout full tidal cycles of varying tidal and hydrological conditions are therefore needed for this. We therefore suggest repeating similar observations during specific conditions, such as spring/neap and high discharge/storm surge conditions. Such measurements would enable to widen the range of tidal and hydrological conditions investigated in relation to plastic transport.

4.3 Delivery ratio of plastic is higher than water

We found that, in relative terms, plastic net transport is higher when compared with net discharge rates (d_r of 18% for water flow and 27-32% for all plastic items). Two main explanations can be hypothesized for this difference in delivery ratios. The first postulates that fundamental differences exist between plastic and water transport processes. Factors not directly accounted for in this study, such as wind and different flow mobilization thresholds could impact differently water particles and plastics, and ultimately result in significantly higher delivery ratios of plastic compared to water. The second hypothesis relates to the site- specific dynamics. High temporary entrapment rates of plastics downstream of the measurement site could lead to lower landward transport rates compared to water particles, because a significant portion of items is temporarily stuck.

Hydrometeorological factors, such as different mobilization thresholds, the influence of wind and later flows and sinking/resuspension mechanisms along the water columns might explain the higher delivery ratios of plastic compared to water particles. Our analysis showed that during the flood phase of the tide, less plastic items were transported in the landward direction compared to water particles. This is somewhat surprising given that the flood phase of the tidal cycle generally corresponds to rising water levels, which could potentially mobilize items that were deposited during falling water levels (ebb phase). However, the lower flow velocities measured during the flood phase compared to the ebb phase of the tidal cycle (-0.23 vs 0.34 m s^{-1}) could explain that a lower share of plastic items reaches their critical threshold of motion, in contrast with water particles. This could be particularly relevant considering that in most rivers, including the Saigon river, plastic items are often

https://doi.org/10.5194/egusphere-2022-1495
Preprint. Discussion started: 1 March 2023

temporarily trapped in floating vegetation, banks or within fluvial structures (Ledieu et al., 2022; Schreyers et al., 2021; van Emmerik et al., 2022c). Quantification of mobilization thresholds of plastics in various entrapment conditions is required to further investigate this mechanism. Besides flow velocity and discharge, wind, waves and lateral flows could influence the drift current speed of plastic items (Laxague et al., 2017; van der Mheen et al., 2020). These factors could generate accelerating or decelerating effects in the propagation of plastic in the river. It is possible that accelerating forces dominated during the ebb phase and decelerating forces during the flood phase. Ultimately, this would result in higher transport distances of plastic items and higher net export rates during the ebb phase. In addition, our study only measured floating plastic transport and therefore tidal dynamics on sub-surface plastic and transfer of plastics between the surface and the deeper layers (sinking and re-suspension) were ignored. This is mainly due to the lack of measurement methods easy to deploy to quantify the distribution of plastic throughout the water column in rivers at a high temporal frequency. Tidal dynamics could also affect the vertical distribution of plastic items, due to variations in water depths and vertical mixing of fresh and salt water (Vermeiren et al., 2016). Ultimately, sinking and re-suspension mechanisms could also contribute to the higher downstream transport rate found for plastic in comparison to water.

Another hypothesis pertains to the local characteristics of our case-study area. High rates of plastic entrapment/deposition downstream of the measurement site, compared to upstream could explain the relative lower landward transport rates compared to water particles. High concentrations of items were often found downstream of the measurement site, due to the presence of docks, piers and jetties which temporarily trap items (Lotcheris et al., 3001in preparation). Similar trapping elements were not found directly upstream of the measurement site. Other factors such as the vegetation, wood jams and meandering might also influence plastic accumulation rates on riverbanks, as already evidenced by recent research (Ledieu et al., 2022; Liro et al., 2020)). The two hypotheses presented for higher delivery ratios of plastics compared to water could be tested using Lagrangian approaches, in combination with high frequency hydrometeorological measurements throughout tidal cycles. Lagrangian studies on plastic transport could provide insights on the (re)mobilization and entrapment thresholds in relation to flow and other hydrometeorological factors such as wind. To the best of our knowledge, no Lagragian-based approaches have so far quantified thresholds of mobilization and stopping of mobile plastics. In addition, Lagrangian approaches are also useful in mapping entrapment/accumulation zones along a river course (Ledieu et al., 2022).

4.4 Plastic transport processes are affected by the geometry, size and buoyancy of items

Our results show that different plastic categories have highly variable net transport rates, depending on items type characteristics, such as size, rigidity and buoyancy. Large and highly buoyant plastics were found to have higher downstream net transport rates than smaller and more neutrally buoyant items. PET items (mainly bottles) were the largest category of plastics by size (average size: 20 cm vs 11 for all item categories) and had the highest delivery ratio found (62%). Highly buoyant items such as EPS and PS items (food containers, isolation foam, cups and plates), with densities comprised between 0.016 to 0.640 g cm^3 for EPS and 1.01 and 1.04 g cm^3 for PS (van Emmerik and Schwarz, 2020) were found to have high downstream net transport rates (39% and 31%, respectively). Such items are also more prone to wind influence (Jackson, 1998; Schwarz et al., 2019). This could cause both deposition effects on the sides of the river or on the riverbanks, or longer travel distances over the

https://doi.org/10.5194/egusphere-2022-1495
Preprint. Discussion started: 1 March 2023

same duration than other items, depending on the wind direction and magnitude. Ryan (2021); A.G.López et al. (2020) found that highly buoyant plastics travel longer distances between the coast and the marine environment. In addition, because of their high buoyancy, these items do not sink easily in the water column (Schwarz et al., 2019). All these factors could explain the higher net export ratios found for highly buoyant plastics. In comparison, more neutrally buoyant and soft items such as PO_{soft} (bags and foils) and Multilayer items (food wrapping) (van Emmerik et al., 2019) had lower net transport rates than average (between 11% and 17% vs 27% for all plastics). Because of their lower buoyancy, such items are more prone to vertical mixing and the influence of changes in turbulence and density fronts, such as salt concentrations (Acha et al., 2003; Ballent et al., 2012). This is particularly relevant for tidal rivers and estuaries, due to changes in the relative balance between fresh and salt water and higher turbulence resulting from the changes in density distribution, compared to the freshwater reaches of the river.

These findings confirm that, similarly to sediment, plastic transport processes should be studied in relation to items characteristics, instead of considering plastics as a single material (Kooi et al., 2018; Schwarz et al., 2019). The wide range of sizes, geometry, densities, buoyancy and masses of plastics strongly impacts their transport dynamics (both vertically and horizontally), as already pointed out by several studies (Ryan, 2021; Waldschläger and Schüttrumpf, 2019; Kuizenga et al., 2021). Comparably, sediment grain size distribution and density strongly influence settling and advection velocities of particles in the water. Recent sediment transport models that incorporated a broader distribution range of grain sizes and densities led to improved estimates of suspended sediment loads compared to models which used more uniform distributions (Lepesqueur et al., 2019).

5 Conclusions

For the first time, we quantified net plastic transport over full tidal cycles in a tidal river using a Eulerian approach. Over this time-period, we conducted sub-hourly measurements of flow velocity, water depth and plastic transport. Time-series of flow velocity and discharge estimates were extrapolated by fitting the tidal constituents of our observations, for which we found that the semi-diurnal and diurnal components were the most significant. We introduced a simple Eulerian approach, which expresses net transport by establishing a balance between the flood (landward) and ebb (seaward) water flows and plastic transport. This approach could easily be transferred to other river systems as it requires limited and affordable equipment.

Four main findings on plastic transport in tidal regions are highlighted from our study. First, net plastic transport is limited compared to total transport, due to changes in flow velocity and direction mainly governed by semi-diurnal tidal cycles. In our case-study, we found that net transport amounted to only 27-32% of the total plastic transport. Secondly, estimates of river plastic transport are highly variable, depending on the tidal dynamics. Diurnal inequality in the tides causes an alternation between cycles with positive net transport (seaward plastic transport) and cycles with negative net transport (i.e.: landward plastic transport). We also found that peak and averaged semidiurnal net transport rates varied by as much as one order of magnitude. Thirdly, net plastic transport shows higher net downstream transport compared to water. We found that net water discharge amounted to 18% of the total river discharge, whereas net plastic transport corresponds to 27-32% of the total plastic transport. This suggests that either plastic travel longer distances than water particles, possibly due to the influence of other

https://doi.org/10.5194/egusphere-2022-1495
Preprint. Discussion started: 1 March 2023

environmental drivers such as wind, or that plastics are get often entrapped downstream from the measurement site, limiting their transport upstream during the flood tidal phase. Lastly, plastics are not uniformly affected by tidal dynamics. Larger and highly buoyant items, such as plastic foams and polystyrene have larger net transport ratios compared to neutrally buoyant and more flexible items, such as bags, foils and food packaging.

With our paper, we show that tidal dynamics play a crucial role in total and net plastic transport in tidal rivers. Bidirectional flows resulting from the semi-diurnal tidal component lead to a large discrepancy between net and total plastic transport rates. With each river that flows into the ocean being affected by tidal dynamics, such effects cannot be neglected anymore in studies that quantify (global) plastic emissions into the ocean. Efforts to both conceptualize and integrate tidal dynamics in river plastic transport and emissions models are therefore required.

Appendix A: Relation between river discharge and flow velocity

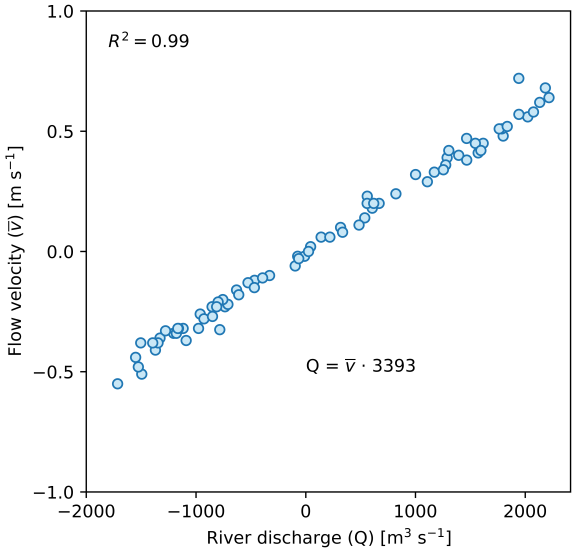

Figure A1. Relation between river discharge and flow velocity. p-value was found to be below <0.01.

Appendix B: Tidal constituent analysis

We found M2 (principal lunar semi-diurnal) and K1 (lunar diurnal) to be the dominating tidal constituents over our flow velocity time-series (Table B1). However, the distortions of the sinusoidal symmetry (Fig.3) could be attributed to shallow water override components (M4 and M6), which were also found to be significant and/or the interactions between the M2 and K1 components (Hoitink et al., 2003; Gatto et al., 2017).

https://doi.org/10.5194/egusphere-2022-1495
Preprint. Discussion started: 1 March 2023

Table B1. Tidal constituent coefficients (amplitude and frequency) and signal-to-noise ratio

Tidal constituent	Symbol	Amplitude [m s^{-1}]	Frequency [cycles $hour^{-1}$]	Signal-to-Noise ratio [-]
Principal lunar semi-diurnal	M2	0.43	0.081	690
Lunar diurnal	K1	0.14	0.042	11000
Fifth diurnal	2MK5	0.050	0.20	27
Shallow water overtide of principal lunar	M4	0.041	0.16	6.6
Shallow water overtide of principal lunar	M6	0.034	0.24	78
Seventh diurnal	3MK7	0.020	0.28	4.5
Lunar terdiurnal	M3	0.011	0.12	1.2
Shallow water eight diurnal	M8	0.0015	0.32	0.15

Appendix C: Relation between river discharge and plastic transport

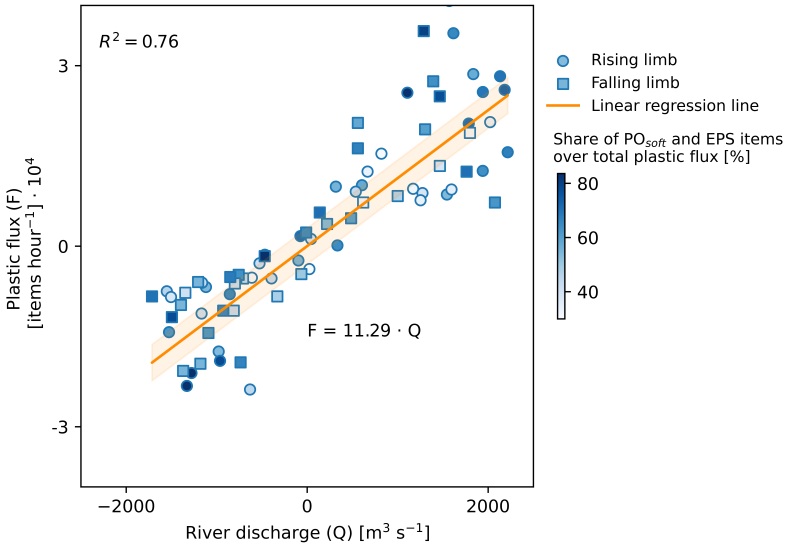

Figure C1. Relation between plastic transport and river discharge. p-value < 0.01.

https://doi.org/10.5194/egusphere-2022-1495
Preprint. Discussion started: 1 March 2023

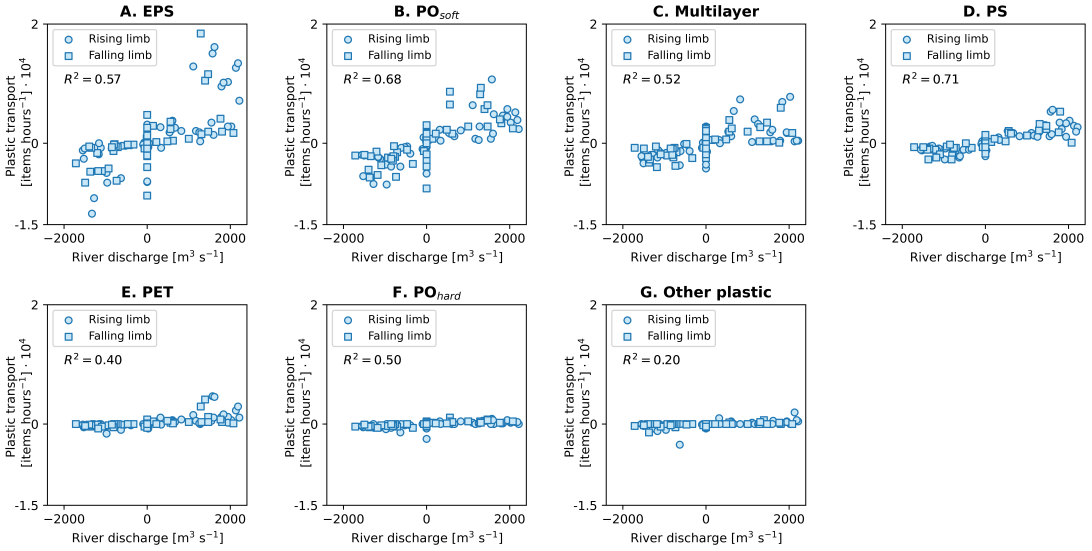

Figure C2. Relation between plastic transport and river discharge by plastic types (A-G). All p-values were found to be below <0.01.

https://doi.org/10.5194/egusphere-2022-1495
Preprint. Discussion started: 1 March 2023

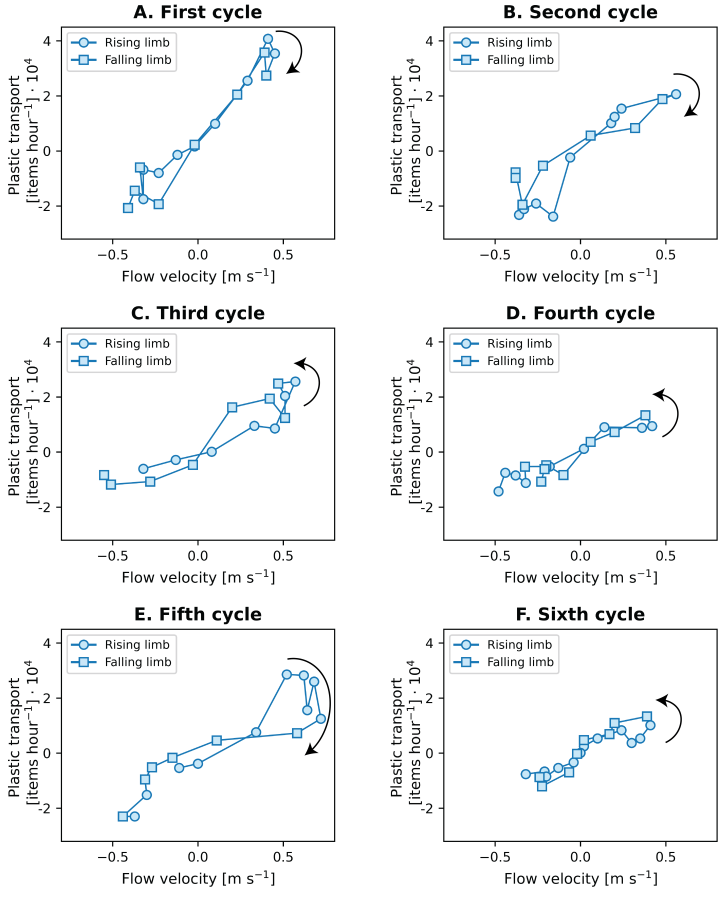

Figure C3. Relation between plastic transport and flow velocity per tidal cycle (A-F). The arrows indicate the direction of the hysteresis between rising and falling limbs of the tidal cycle

https://doi.org/10.5194/egusphere-2022-1495
Preprint. Discussion started: 1 March 2023

Appendix D: Additional statistics for plastic transport

Table D1. Plastic transport, flow velocity and discharge per tidal cycle. Plastic transport are reported in both items transport and mass transport.

		Plastic transport			Flow velocity	River discharge
Cycle	**Variables**	**Items transport [items hours^{-1}]**	**Mass transport (median mass) [kg day^{-1}]**	**Mass transport (mean mass) [kg day^{-1}]**	**[m.s^{-1}]**	**[m^3.s^{-1}]**
1	Ebb (f_{ebb})	$2.6 \cdot 10^4$	$3.1 \cdot 10^3$	$6.3 \cdot 10^3$	0.40	1400
	Flood (f_{flood})	$-8.9 \cdot 10^3$	-9.2 x 10^2	$-2.1 \cdot 10^3$	-0.26	-870
	Net (f_{net})	1.1 x 10^4	$1.4 \cdot 10^3$	$2.6 \cdot 10^3$	0.11	380
	Delivery ratio (d_r) [%]	58	63	58	33	33
2	Ebb (f_{ebb})	$1.4 \cdot 10^4$	$1.5 \cdot 10^3$	$3.4 \cdot 10^3$	0.22	740
	Flood (f_{flood})	$-1.2 \cdot 10^4$	$-1.1 \cdot 10^3$	$-2.8 \cdot 10^3$	-0.24	-810
	Net (f_{net})	$-1.9 \cdot 10^3$	$-1.7 \cdot 10^1$	$-3.4 \cdot 10^2$	-0.0056	-190
	Delivery ratio (d_r) [%]	-15	-1	-11	-24	-24
3	Ebb (f_{ebb})	$1.6 \cdot 10^4$	1.6 x 10^3	$3.8 \cdot 10^3$	0.42	1400
	Flood (f_{flood})	$-6.7 \cdot 10^3$	$-6.6 \cdot 10^2$	$-1.6 \cdot 10^3$	-0.23	-770
	Net (f_{net})	$6.1 \cdot 10^3$	$6.0 \cdot 10^2$	$1.4 \cdot 10^3$	0.14	470
	Delivery ratio (d_r) [%]	51	51	50	41	41
4	Ebb (f_{ebb})	$7.1 \cdot 10^3$	$8.3 \cdot 10^2$	$1.8 \cdot 10^3$	0.24	800
	Flood (f_{flood})	$-7.0 \cdot 10^3$	$-7.3 \cdot 10^2$	$-1.7 \cdot 10^3$	-0.23	-790
	Net (f_{net})	$-1.0 \cdot 10^3$	$-6.4 \cdot 10^1$	$-2.3 \cdot 10^2$	-0.0034	-120
	Delivery ratio (d_r) [%]	-14	-8	-13	-14	-14
5	Ebb (f_{ebb})	$1.6 \cdot 10^4$	$1.7 \cdot 10^3$	$3.8 \cdot 10^3$	0.42	1400
	Flood (f_{flood})	$-4.2 \cdot 10^3$	$-5.3 \cdot 10^2$	$-1.1 \cdot 10^3$	-0.21	-710
	Net (f_{net})	$7.7 \cdot 10^3$	$7.9 \cdot 10^2$	$1.7 \cdot 10^3$	0.15	520
	Delivery ratio (d_r) [%]	69	64	66	46	46
6	Ebb (f_{ebb})	$6.4 \cdot 10^3$	$7.0 \cdot 10^2$	$1.5 \cdot 10^3$	0.26	880
	Flood (f_{flood})	$-1.1 \cdot 10^4$	$-1.0 \cdot 10^3$	$-2.4 \cdot 10^3$	-0.23	-780
	Net (f_{net})	$-2.9 \cdot 10^3$	$-2.3 \cdot 10^2$	$-6.3 \cdot 10^2$	-0.075	-25.6
	Delivery ratio (d_r) [%]	-33	-26	-31	-3	-3
All cycles	Ebb (f_{ebb})	$1.5 \cdot 10^4$	$1.7 \cdot 10^3$	$3.6 \cdot 10^3$	0.34	1100
	Flood (f_{flood})	$-8.6 \cdot 10^3$	$-8.3 \cdot 10^2$	$-2.0 \cdot 10^3$	-0.23	-790
	Net (f_{net})	$3.1 \cdot 10^3$	$4.0 \cdot 10^2$	$7.6 \cdot 10^2$	0.051	170
	Delivery ratio (d_r) [%]	27	32	27	18	18

Table D2. Mean and median mass per item. The mass statistics were taken from van Emmerik et al. (2019). The reported values for Multilayer and Other plastic correspond to the mean and median for all items, since mass was not measured for a sufficient number of items for these two categories

Plastic type	**EPS**	**PO$_{soft}$**	**Multilayer**	**PS**	**PET**	**PO$_{hard}$**	**Other plastic**
Mean mass per item [g]	7.0	11	10	11	20	12	10
Median mass per item [g]	1.9	2.9	4.3	6.0	21	7.7	4.3

https://doi.org/10.5194/egusphere-2022-1495
Preprint. Discussion started: 1 March 2023

Author contributions. Conceptualization: LS and TvE; Investigation - Data collection: LS, TvE, KB, KvLT; Formal analysis: LS; Visualization: LS; Data curation: LS; Writing-original draft: LS; Writing-reviewing and editing: all authors; Supervision: MvdP; Project administration: TvE and LS; Funding acquisition: TvE and LS.

Competing interests. The authors declare having no competing interests

Acknowledgements. Thank you to Quynh Nhu, Thanh Phng, My Linh, Do Tien, Minh Son, Quoc Dung, Hoang Linh, Tran Danh, Diem Quynh, Anh Thu, Phuong Uyen and Thu Trúc for their help in data collection. Thank you to Henk Jongbloed, Joris Beemster, Nick Wallerstein and Ton Hoitink for their meaningful inputs on the manuscript. The work of LS was supported by the Discovery Element of the European Space Agency's Basic Activities (ESA contract no. 4000132682/20/NL/GLC). The work of TvE was supported by the Veni Research Program, the River Plastic Monitoring Project with project number 18211, which was (partly) financed by the Dutch Research Council (NWO).

Data availability

The data underlying this manuscript will be made available upon publication at: 10.4121/21732818. For reviewers, the dataset is already accessible at: https://figshare.com/s/84ba02a91b8d1864ab48.

https://doi.org/10.5194/egusphere-2022-1495
Preprint. Discussion started: 1 March 2023

References

Acha, E., Mianzan, H., Iribarne, O., Gagliardini, D., Lasta, C., and Daleo, P.: The role of the Rıo de la Plata bottom salinity front in accumulating debris, Marine Pollution Bulletin, 46, 197–202, 2003.

A.G.López, Najjar, R., Friedrichs, M., Hickner, M., and Wardrop, D.: Estuaries as Filters for Riverine Microplastics: Simulations in a Large, Coastal-Plain Estuary, Frontiers in Marine Science, 8, 2055, 2020.

Ballent, A., Pursuer, A., de Jesus Mendes, P., Pando, S., and Thomsen, L.: Physical transport properties of marine microplastic pollution, Biogeosciences Discussion, 9, 18 755–18 798, 2012.

Ballio, F., Pokrajac, D., Radice, A., and Sadabadi, S. H.: Lagrangian and Eulerian description of bed load transport, Journal of Geophysical Research: Earth Surface, 123, 384–408, 2018.

Beaumont, N., Aanesen, M., Börger, M., Clark, J., Cole, M., Hooper, T., Lindeque, P., Pascoe, C., and Wyles, J.: Global ecological, social and economic impacts of marine plastic, Marine Pollution Bulletin, 142, 189–195, 2019.

Borrelle, S., Rochman, C., Liboiron, M., Bond, A., Luscher, A., Bradshaw, H., and Provencher, J.: Why we need an international agreement on marine plastic pollution, Proceedings of the National Academy of Sciences, 114, 9994–9997, 2017.

Camenen, B., Gratiot, N., J.-A., C., Tran, F., Nguyen, A.-T., Dramais, G., van Emmerik, T., and Némery, J.: Monitoring discharge in a tidal river using water level observations: Application to the Saigon River, Vietnam, Science of the Total Environment, 761, 2021.

Codiga, D.: Unified Tidal Analysis and Prediction Using the UTide Matlab Functions. Technical Report 2011-01., Tech. rep., Graduate School of Oceanography, University of Rhode Island, Narragansett, RI, 2011.

Delorme, A., Koumba, G., Roussel, E., Delor-Jestin, F., Peiry, J.-L., and et al., O. V.: The life of a plastic butter tub in riverine environments, Environmental Pollution, 287, 117 656, 2010.

Fernandes, S. and Pillay, S.: A study of the net transport of nitrates from estuaries of the eThekwini Municipality of Durban, KwaZulu-Natal, South Africa, Environmental Earth Sciences, 67, 2193–2203, 2010.

Fernandino, G., Elliff, C., Frutuoso, G., da Silva, E. N. M., Gama, G. S., de Oliveira Sousa, J., and Silva, I. R.: Considerations on the effects of tidal regimes in the movement of floating litter in an estuarine environment: Case study of the estuarine system of Santos-São Vicente, Brazil, Marine Pollution Bulletin, 110, 2016.

Gatto, V., van Prooijen, B., and Wang, Z.: Net sediment transport in tidal basins: quantifying the tidal barotropic mechanisms in a unified framework, Ocean Dynamics, 67, 1385–1406, 2017.

Gisen, J. and Savenije, H.: Estimating bankfull discharge and depth in ungauged estuaries,, Water Resources Research, 51, 2015.

González-Fernández, D. and Hanke, G.: Toward a harmonized approach for monitoring of riverine floating macro litter inputs to the marine environment, Frontiers in Marine Science, 4, 86, 2017.

González-Fernández, D., Cózar, A., Hanke, G., Viejo, J., Morales-Caselles, C., Bakiu, R., Barceló, D., Bessa, F., Bruge, A., Cabrera, M., et al.: Floating macrolitter leaked from Europe into the ocean, Nature Sustainability, 4, 474–483, 2021.

Healy, R., Winter, T., LaBaugh, J., and Franke, O.: Water budgets: foundations for effective water-resources and environmental management, Tech. rep., U.S. Geological Survey, 2007.

Hoitink, A. and Jay, D.: Tidal river dynamics: Implications for deltas, Reviews of Geophysics', 54, 240–272, 2016.

Hoitink, A., Hoekstra, P., and van Maren, D.: Flow asymmetry associated with astronomical tides: Implications for the residual transport of sediment, Journal of Geophysical Research: Oceans, 108, 2003.

https://doi.org/10.5194/egusphere-2022-1495
Preprint. Discussion started: 1 March 2023

Hurley, R., Woodward, J., and Rothwell, J. J.: Microplastic contamination of river beds significantly reduced by catchment-wide flooding, Nature Geoscience, 11, 251–257, 2018.

Jackson, L. T. . N.: Spatial and temporal variations in debris accumulation and composition on an estuarine shoreline, Cliffwood Beach, New Jersey, USA, Marine Pollution Bulletin, 36, 705–711, 1998.

Jambeck, J. R., Geyer, R., Wilcox, C., Siegler, T. R., Perryman, M., Andrady, A., Narayan, R., and Law, K. L.: Plastic waste inputs from land into the ocean, Science, 347, 768–771, https://doi.org/10.1126/science.1260352, publisher: American Association for the Advancement of Science (AAAS), 2015.

Koelmans, A., Ellen, B., Foekema, E., Kooi, M., Mintenig, S., Ossendorp, B., Redondo-Hasselerharm, P., Verschoor, A., van Wezel, A., and Scheffer, M.: Risks of Plastic Debris: Unravelling Fact, Opinion, Perception, and Belief, Environmental Science & Technology, 51, 11 513–11 519, 2021.

Kooi, M., Besseling, E., Kroeze, C., van Wezel, A., and Koelmans, A.: Modeling the Fate and Transport of Plastic Debris in Freshwaters: Review and Guidance., in: Freshwater Microplastics. The Handbook of Environmental Chemistry, edited by Wagner, M. and Lambert, S., vol. 51, 2018.

Kuizenga, B., van Emmerik, T., Waldschläger, K., and Kooi, M.: Will it Float? Rising and Settling Velocities of Common Macroplastic Foils, Environmental Science & Technology Water, 2, 975–981, 2021.

Lahens, L., Strady, E., Kieu-Le, T.-C., Dris, R., Boukerma, K., Rinnerte, E., Gasperi, J., and Tassin, B.: Macroplastic and microplastic contamination assessment of a tropical river (Saigon River, Vietnam) transversed by a developing megacity, Environmental Pollution, 235, 1–10, 2018.

Laxague, N., Özgökmen, T. M., Brian, K., Novelli, G., Shcherbina, A., Sutherland, P., Guigand, C., Lund, B., Mehta, S., Alday, M., and Molemaker, J.: Observations of Near-Surface Current Shear Help Describe Oceanic Oil and Plastic Transport, Geophysical Research Letters', 45, 245–249, 2017.

Lebreton, L. C., Van Der Zwet, J., Damsteeg, J.-W., Slat, B., Andrady, A., and Reisser, J.: River plastic emissions to the world's oceans, Nature communications, 8, 1–10, 2017.

Ledieu, L., Tramoy, R., Mabilais, D., Ricordel, S., Verdier, L., Tassin, B., and Gasperi, J.: Macroplastic transfer dynamics in the Loire estuary: Similarities and specificities with macrotidal estuaries, Marine Pollution Bulletin, 182, 2022.

Lepesqueur, J., Hostache, R., Martínez-Carreras, N., Montargès-Pelletier, E., and Hissler, C.: Sediment transport modelling in riverine environments: on the importance of grain-size distribution, sediment density, and suspended sediment concentrations at the upstream boundary, Hydrology and Earth Systems Science, 23, 3901–3915, 2019.

Liro, M., van Emmerik, T., Wy\.zga, B., Liro, J., and Mikuś, P.: Macroplastic Storage and Remobilization in Rivers, Water, 12, 2055, https://doi.org/10.3390/w12072055, publisher: Multidisciplinary Digital Publishing Institute AG, 2020.

Lotcheris, R., Schreyers, L., and van Emmerik, T.: Macroplastics in a tidal river: Lagrangian observations of trapping, transport, and remobilisation, Journal of Nothingness, 3001in preparation.

Meijer, L. J., van Emmerik, T., van der Ent, R., Schmidt, C., and Lebreton, L.: More than 1000 rivers account for 80% of global riverine plastic emissions into the ocean, Science Advances, 7, eaaz5803, 2021.

Nguyen, D. and Nguyen, D.: A simple approach to estimating freshwater discharge in branched estuarine systems. Hydrological processes, Hydrological processes, 32, 2018.

Nguyen, H., Nguyen, H., Quang, N., Hieu, N. D., and Thang, L.: Spatio-temporal pattern of water quality in the Saigon-Dong Nai river system due to waste water pollution sources, International Journal of River Basin Management, 19, 221–243, 2021.

https://doi.org/10.5194/egusphere-2022-1495
Preprint. Discussion started: 1 March 2023

Nguyen, T., Némery, J., Gratiot, N., Garnier, J., Strady, E., Nguyen, P. D., Tran, V., Nguyen, A., S. Tung Cao, S., and Huynh, T.: Nutrient budgets in the Saigon–Dongnai River basin: Past to future inputs from the developing Ho Chi Minh megacity (Vietnam), River Research and Applications, 36, 2020.

Rantz, S.: Measurement and Computation of Streamflow: Volume 1. Measurement of Stage and Discharge, Tech. rep.

Rochman, C., Cook, A.-M., and Koelmans, A.: Plastic debris and policy: Using current scientific understanding to invoke positive change, Environmental Toxicology and Chemistry, 35, 1617–1626, 2016.

Roebroek, C. T., Harrigan, S., Van Emmerik, T. H., Baugh, C., Eilander, D., Prudhomme, C., and Pappenberger, F.: Plastic in global rivers: are floods making it worse?, Environmental Research Letters, 16, 025 003, 2021a.

Roebroek, C. T., Laufkötter, C., González-Fernández, D., and van Emmerik, T.: The quest for the missing plastics: Large uncertainties in river plastic export into the sea, Environmental Pollution, 312, 119 948, https://doi.org/10.1016/j.envpol.2022.119948, 2022.

Roebroek, C. T. J., Hut, R., Vriend, P., Winter, W. d., Boonstra, M., and Emmerik, T. H. M. v.: Disentangling Variability in Riverbank Macrolitter Observations, Environmental Science &amp$\mathsemicolon$ Technology, 55, 4932–4942, https://doi.org/10.1021/acs.est.0c08094, publisher: American Chemical Society (ACS), 2021b.

Ryan, P.: Does size and buoyancy affect the long-distance transport of floating debris?, Environmental Research Letters, 10, https://doi.org/10.1016/j.ecss.2021.107186, 2021.

Ryan, P. G. and Perold, V.: Limited dispersal of riverine litter onto nearby beaches during rainfall events, Estuarine, Coastal and Shelf Science, 251, 107 186, https://doi.org/10.1016/j.ecss.2021.107186, publisher: Elsevier BV, 2021.

Schmidt, C., Krauth, T., and Wagner, S.: Export of plastic debris by rivers into the sea, Environmental science & technology, 51, 12 246–12 253, 2017.

Schreyers, L., van Emmerik, T., Luan Nguyen, T., Castrop, E., Phung, N.-A., Kieu-Le, T.-C., Strady, E., Biermann, L., and van der Ploeg, M. J.: Plastic plants: The role of water hyacinths in plastic transport in tropical rivers, Frontiers in Environmental Science, 9, 177, 2021.

Schwarz, A., Ligthart, T., Boukris, E., and van Harmelen, T.: Sources, transport, and accumulation of different types of plastic litter in aquatic environments: A review study, Marine Pollution Bulletin, 143, 92–100, https://doi.org/https://doi.org/10.1016/j.marpolbul.2019.04.029, 2019.

Sutton, R., Mason, S., Stanek, S., Willis-Norton, E., Wren, I., and Box, C.: Microplastic contamination in the San Francisco Bay, California, USA, Marine Pollution Bulletin, 109.

Tasseron, P., Begemann, F., Joosse, N., van der Ploeg, M., van Driel, J., and van Emmerik, T.: Urban water systems as entry points for river plastic pollution, Environmental Science and Pollution Research, 3001under review.

Tessler, Z., C.J.Vörösmarty, Overeem, I., and Syvitzki, J.: A model of water and sediment balance as determinants of relative sea level rise in contemporary and future deltas, Geomorphology, 305, 2019–220, 2018.

Tramoy, R., Gasperi, J., Colasse, L., Silvestre, M., Dubois, P., Noûs, C., and Tassin, B.: Transfer dynamics of macroplastics in estuaries – New insights from the Seine estuary: Part 2. Short-term dynamics based on GPS-trackers, Marine Pollution Bulletin, 160, 111 566, https://doi.org/10.1016/j.marpolbul.2020.111566, publisher: Elsevier BV, 2020a.

Tramoy, R., Gasperi, J., Colasse, L., and Tassin, B.: Transfer dynamic of macroplastics in estuaries — New insights from the Seine estuary: Part 1. Long-term dynamic based on date-prints on stranded debris, Marine Pollution Bulletin, 152, 110 894, https://doi.org/10.1016/j.marpolbul.2020.110894, publisher: Elsevier BV, 2020b.

Valero, D., Belay, B. S., Moreno-Rodenas, A., Kramer, M., and Franca, M. J.: The key role of surface tension in the transport and quantification of plastic pollution in rivers, Water Research, 226, 119 078, https://doi.org/https://doi.org/10.1016/j.watres.2022.119078, 2022.

https://doi.org/10.5194/egusphere-2022-1495
Preprint. Discussion started: 1 March 2023

van der Mheen, M., Pattiaratchi, C., Cosoli, S., and Wandres, M.: Depth-Dependent Correction for Wind-Driven Drift Current in Particle Tracking Applications, Frontiers in Marine Science, 7, 2020.

van Emmerik, T. and Schwarz, A.: Plastic debris in rivers, Water, 7, e1398, 2020.

van Emmerik, T., Strady, E., Kieu-Le, T.-C., Nguyen, L., and Gratiot, N.: Seasonality of riverine macroplastic transport, Scientific reports, 9, 1–9, 2019.

van Emmerik, T., de Lange, S., Frings, R., Schreyers, L., Aalderink, H., Leusink, J., Begemann, F., Hamers, E., Hauk, R., Janssens, N., et al.: Hydrology as a driver of floating river plastic transport, Earth's Future, 10, e2022EF002 811, 2022a.

van Emmerik, T., Frings, R., Schreyers, L., Hauk, R., de Lange, S., and Mellink, Y.: River plastic during floods: Amplified mobilization, limited river-scale dispersion, preprint on ResearchSquare, 2022b.

van Emmerik, T., Mellink, Y., Hauk, R., Waldschläger, K., and Schreyers, L.: Rivers as plastic reservoirs, Frontiers in Water, p. 212, 2022c.

Vermeiren, P., Muñoz, C., and Kou, I.: Sources and sinks of plastic debris in estuaries: A conceptual model integrating biological, physical and chemical distribution mechanisms, Marine Pollution Bulletin, 113, 7–16, 2016.

Vriend, P., Van Calcar, C., Kooi, M., Landman, H., Pikaar, R., and Van Emmerik, T.: Rapid assessment of floating macroplastic transport in the Rhine, Frontiers in Marine Science, 7, 10, 2020.

Waldschläger, K. and Schüttrumpf, H.: Effects of Particle Properties on the Settling and Rise Velocities of Microplastics in Freshwater under Laboratory Conditions, Environmental Science & Technology, 53, 1958–1966, 2019.

Waldschläger, K., Brückner, M. Z., Carney Almroth, B., Hackney, C. R., Adyel, T. M., Alimi, O. S., Belontz, S. L., Cowger, W., Doyle, D., Gray, A., Kane, I., Kooi, M., Kramer, M., Lechthaler, S., Michie, L., Nordam, T., Pohl, F., Russell, C., Thit, A., Umar, W., Valero, D., Varrani, A., Warrier, A. K., Woodall, L. C., and Wu, N.: Learning from natural sediments to tackle microplastics challenges: A multidisciplinary perspective, Earth-Science Reviews, 228, 104 021, https://doi.org/https://doi.org/10.1016/j.earscirev.2022.104021, 2022.